

Medd. 26, No. 14 (1952).

<sup>6</sup>A. Bohr and B. R. Mottelson, Kgl. Danske Videnskab. Selskab, Mat.-Fys. Medd. 27, No. 16 (1953).

<sup>7</sup>K. Heyde and P. J. Brussaard, Nucl. Phys. A104, 81 (1967).

<sup>8</sup>V. K. Thankappan and S. P. Pandya, Nucl. Phys. 39, 394 (1962).

<sup>9</sup>B. Castel, K. W. C. Stewart, and M. Harvey, to be published.

<sup>10</sup>B. Castel, K. W. C. Stewart, and M. Harvey, Can. J. Phys. 47, 1490 (1970).

<sup>11</sup>S. I. Baker and R. E. Segel, Phys. Rev. 170, 1046 (1968).

<sup>12</sup>L. Meyer-Schützmeister, D. S. Gemmell, R. E. Holland, F. T. Kuchnir, H. Ohnuma, and N. G. Puttaswamy, Phys. Rev. 187, 1210 (1969); C. F. Monahan, H. C. Evans, J. H. Montague, W. R. Paulson, and W. Zuk, Can. J. Phys. 48, 2683 (1970).

<sup>13</sup>B. H. Wildenthal and E. Newman, Phys. Letters 28B, 108 (1968).

<sup>14</sup>B. H. Wildenthal, quoted in H. Ohnuma, F. T. Kuchnir, D. S. Gemmell, R. E. Holland, L. Meyer-Schützmeister, and N. G. Puttaswamy, Nucl. Phys. A149, 141 (1970).

<sup>15</sup>T. T. S. Kuo, Nucl. Phys. A103, 71 (1967).

<sup>16</sup>Ohnuma, Kuchnir, Gemmell, Holland, Meyer-Schützmeister, and Puttaswamy, Ref. 14.

<sup>17</sup>J. L. Durell and R. D. Symes, Phys. Letters 31B, 358 (1970).

<sup>18</sup>A. N. James, J. F. Sharpey-Schaber, P. R. Alderson, D. C. Bailey, J. L. Durell, and M. W. Greene, in *Proceedings of the International Conference on Properties of Nuclear States, Montréal, Canada, 1969* (Presses de l'Université de Montréal, Montréal, Canada, 1969).

<sup>19</sup>L. S. Kisslinger and R. A. Sorenson, Rev. Mod. Phys. 35, 853 (1963).

<sup>20</sup>W. P. Beres, Nucl. Phys. 75, 255 (1966).

## Optical-Potential Scattering of Nucleons by Carbon at Medium Energies

Joseph S. Chalmers

*Department of Physics, University of Louisville, Louisville, Kentucky 40208*

(Received 15 October 1970)

The elastic scattering of nucleons by carbon, at incident energies of 142, 210, and 330 MeV, is calculated from an optical potential retaining all terms to second order in the  $N$ - $N$  amplitudes. The amplitudes are calculated using recent  $N$ - $N$  phase-parameter sets obtained by the Yale, Livermore, and Michigan State Groups. Nuclear correlation functions of both the Fermi and Brueckner-Gammel types are used to represent nuclear structure. Comparison with experiment is made in order to distinguish among different  $N$ - $N$  phase-parameter sets, and among different types of nuclear correlation functions.

In earlier work,<sup>1</sup> the elastic scattering of nucleons by light nuclei, at energies of 140 to 310 MeV, was calculated from an optical potential retaining all terms to second order in the two-nucleon amplitudes. The amplitudes were calculated using the YLAN3M-YLAM and L-IV phase-parameter sets of the Yale<sup>2</sup> and Livermore<sup>3</sup> groups, respectively. Since that time, these phase-parameter sets have been superseded by more recent searches.<sup>4-7</sup> It is the purpose of this work to determine the effect of these new phase-parameter sets on the agreement of the calculated nucleon-nuclear observables with experiment and to investigate the degree to which the calculated observables depend on the shape of the nuclear correlation function.

The potential used in this calculation is derived from the Watson<sup>8</sup> formalism. The double-scattering term and an impulse-approximation correction term, both of which are binary in the two-nucleon amplitudes, are retained. The resulting optical potential is used in the numerical solution of the partial-wave integral-scattering equation in momentum space. Details of the calculation are given

in Ref. 1 and elsewhere.<sup>9</sup>

The two-nucleon amplitudes are calculated using the recent Yale<sup>4</sup> and Livermore<sup>5,6</sup> phase-parameter sets at 142, 210, and 330 MeV, and the Michigan State<sup>7</sup> phase-parameter set at 210 MeV.

In Ref. 1, nuclear structure was represented by both Fermi (F) and Brueckner-Gammel (BG) type correlations. For the Fermi type, correlation functions were derived by assuming a Fermi gas of nucleons. For the Brueckner-Gammel case, however, only the correlation length was known, and a form for the correlation function was chosen for convenience. The BG-type function was taken to be

$$G_B = -(1 - \delta r^2/b^2)e^{-r^2/b^2}, \quad (1)$$

subject to the conditions

$$\int G_B d\tau = 0 \quad (2)$$

and

$$\int_0^\infty G_B dr = R_c, \quad (3)$$

with  $R_c = -0.84$  F as determined by Johnston and Watson,<sup>10</sup> from the work of Brueckner and Gammel.<sup>11</sup> From (2),  $\delta = \frac{2}{3}$  and from (3),  $b = 1.42$  F. Since (2) is appropriate for nuclei in which the nuclear radius is much greater than the correlation length, the form (1) subject to (2) and (3) is designated soft core infinite (S.C.I.).

In order to determine the effect of the infinite-nucleus approximation, we used the exact expression for which (2) is an approximation;

$$\int \rho_0(\vec{r}_1)\rho_0(\vec{r}_2)G_B(\vec{r}_1 - \vec{r}_2)d\tau_1d\tau_2 = 0.$$

If a Gaussian density is used, this reduces to

$$\int e^{-r^2/2a^2}G_B(r)d\tau = 0, \quad (4)$$

where  $a$  is the Gaussian range parameter (1.96 F for carbon). If form (1) is used subject to (3) and (4), then  $\delta = 0.95$  and  $b = 1.80$  F. This case is designated soft core finite (S.C.F.).

To explore the effect of a hard core in the correlation function, we used another BG-type function

$$G_B = -1, \quad r < r_c \\ = -[1 - \delta(r - r_c)/b]e^{-(r - r_c)/b}, \quad r > r_c \quad (5)$$

with the core radius  $r_c$  taken to be 0.5 F. For this function, (2) and (3) yield  $\delta = 0.45$  and  $b = 0.62$ .

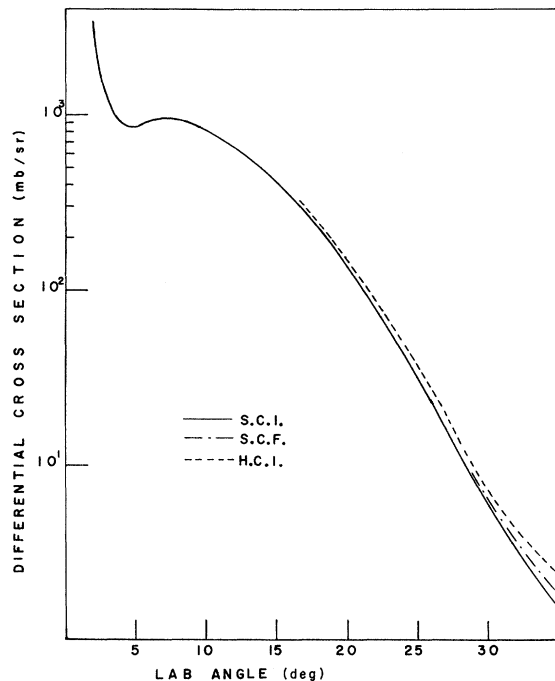


FIG. 1. Differential cross section for  $p$ -C scattering at incident lab energy of 142 MeV as calculated with the L-X phase-parameter set, showing the effects of different BG correlation functions.

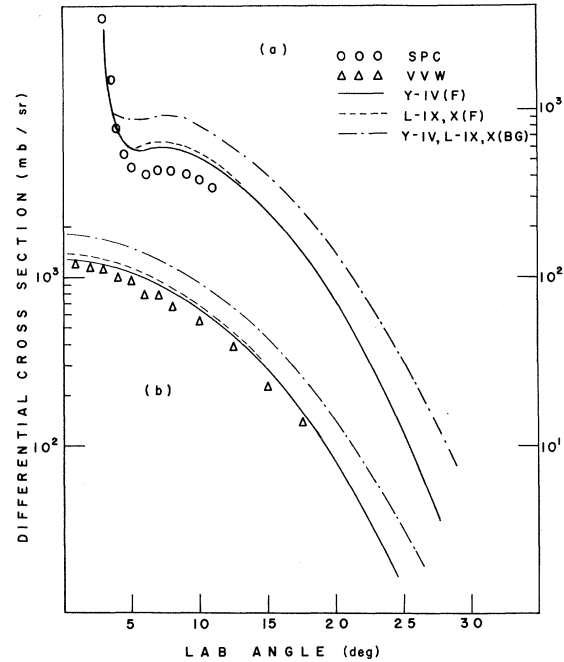


FIG. 2. Calculated differential cross section versus data at incident lab energy of 142 MeV for (a)  $p$ -C, and (b)  $n$ -C elastic scattering.

Form (5) subject to conditions (2) and (3) is designated hard core infinite (H.C.I.).

Figure 1 shows the effect of the different BG correlation forms on the differential cross section at 142 MeV as calculated with the L-X set. As can be seen, the different BG correlation forms have little effect on the differential cross section at 142 MeV, until the first diffraction minimum is reached. At 330 MeV, the curves are virtually indistinguishable and are not plotted. Since these three forms are all required to satisfy (3), these results would indicate that the correlation length is the dominant feature of the nuclear correlation function so far as these calculations are concerned.

In the following calculations, BG refers to the S.C.I. mode:

*Differential cross section 142 MeV.* Figure 2 shows the calculated differential cross section at 142 MeV together with the  $p$ -C data of Steinberg, Palmieri, and Cormack<sup>12</sup> and the  $n$ -C data of VanZyl, Voss, and Wilson.<sup>13</sup> The calculated curves are little affected by the choice of phase-parameter set, but are considerably affected by the type of correlation function used, with the F type giving much better results at this energy than the BG type. As can be seen, the fit to the  $n$ -C data is quite good, while the fit to the  $p$ -C data is less impressive. The difficulty of fitting both  $p$ -C and  $n$ -C differential cross-section data at this en-

ergy, without renormalization of data, has been discussed by Batty.<sup>14</sup>

**210 MeV.** Figure 3 shows the calculated differential cross section at 210 MeV compared with the data of Thwaites.<sup>15</sup> When used in conjunction with the F-type correlation function, the Y-IV and L-X sets fits the data very well, and the L-IX set, only slightly less so. The MS-A set, however, shows excessive Coulomb interference compared to the data. All of the calculated curves with the BG-type correlation function lie about 50% above the data.

**330 MeV.** Figure 4 shows the calculated differential cross section at 330 MeV compared with the 310-MeV  $p$ -C data of Chamberlain *et al.*<sup>16</sup> and the 350-MeV  $n$ -C data of Ashmore, Mather, and Sen.<sup>17</sup> In the  $p$ -C case, there is little splitting among phase-parameter sets in the calculated curves. The  $n$ -C curves, however, show very noticeable splitting among the phase-parameter sets. In each case the different correlation functions are readily distinguishable, with the BG type fitting both data sets very well, particularly when used with the Y-IV phase-parameter set.

**Polarization 142 MeV.** Figure 5(a) shows the calculated polarization against the  $p$ -C data of Dickson and Salter<sup>18</sup> adjusted according to Jarvis and Rose.<sup>19</sup> None of the phase-parameter sets fit the

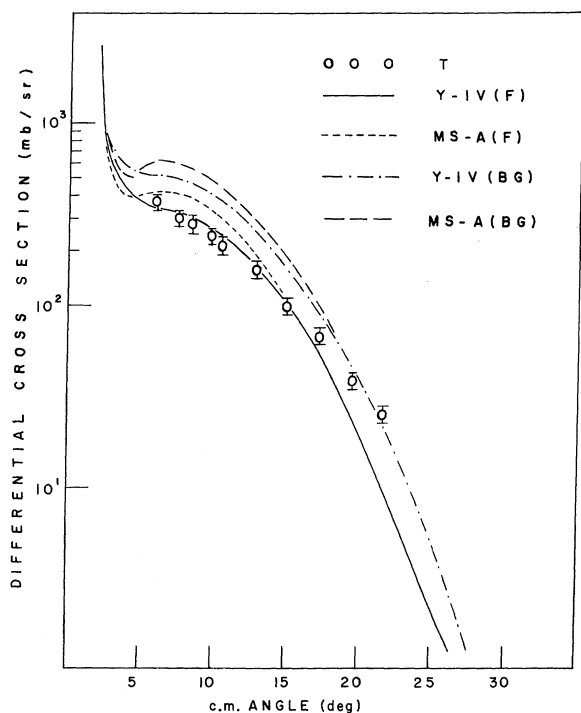


FIG. 3. Calculated differential cross section versus data for  $p$ -C elastic scattering at incident lab energy of 210 MeV.

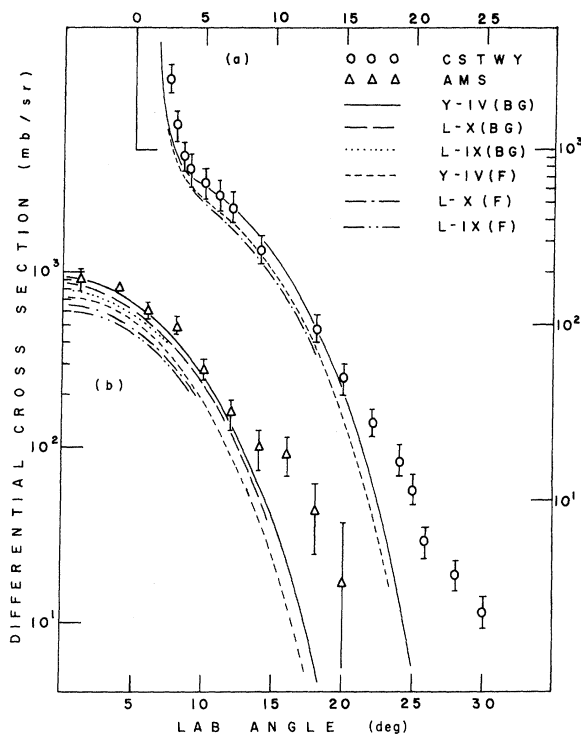


FIG. 4. Calculated differential cross section versus data at incident lab energy of 330 MeV for (a)  $p$ -C, and (b)  $n$ -C elastic scattering.

data quantitatively with either the F- or BG-type correlation functions. Also, as noted elsewhere,<sup>1</sup> the BG-type correlation function does not give rise to the characteristic polarization diffraction minimum whereas the F-type function does.

**210 MeV.** Figure 5(b) shows the polarization against the data of Hafner.<sup>20</sup> Again, there is little splitting among phase-parameter sets, except for MS-A. The fits with the F-type correlation function are qualitatively good over the entire range of the data, while the BG-type correlation gives a polarization minimum which is too shallow.

**330 MeV.** Figure 5(c) shows the calculated polarization at 330 MeV against the data of Chamberlain *et al.*<sup>16</sup> There is again little splitting among phase-parameter sets. The fits are qualitatively poor beyond  $\sim 10^\circ$  with all of the calculated curves overshooting the data in the range  $10$ – $20^\circ$ . While the F- and BG-type correlation functions are readily distinguishable, one cannot choose between them on the basis of these fits at this energy.

The preceding comparison of the calculation with the data clearly shows that the F-type correlation gives a better fit at 142 and 210 MeV than does the BG type, while at 330 MeV it is the BG-type correlation which gives the better fit, in agreement with the conclusion reached in Ref. 1. In addition, the present work has shown that variation of the

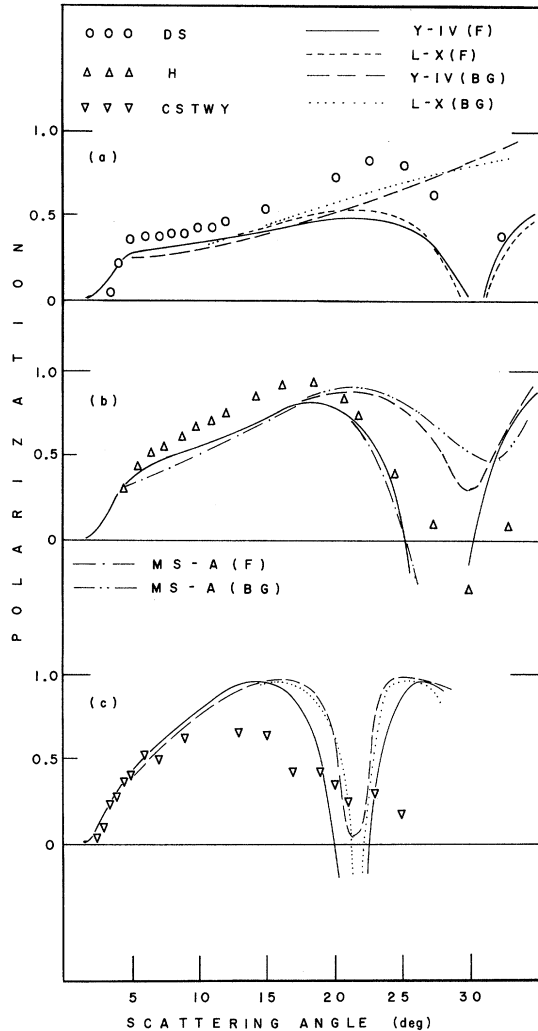


FIG. 5. Calculated polarization versus data for  $p$ -C elastic scattering. (a) 142-MeV incident energy, (b) 210-MeV incident energy, and (c) 330-MeV incident energy. Scattering angle is lab angle for (a) and (c); c.m. angle for (b).

shape of the BG-type correlation function has negligible effect on the calculated observables pro-

vided the correlation length is held fixed. In comparing the calculated differential cross section with experiment at the various energies, one can see that the calculated curves are descending relative to the data with increasing energy. This trend was not apparent in Ref. 1. Preliminary work shows that the BG-type function gives an excellent fit to data at 425 MeV as well as at 330 MeV so that this trend might stabilize above 300 MeV. In any event, we do not have an explanation for this trend.

The splitting among phase-parameter sets in the present work is uniformly reduced from that observed in Ref. 1. This is a consequence of the convergence of the recent searches toward a common phase-parameter set at each energy. It should be noted that the nonnegligible splitting observed at 210 MeV cannot be correlated with any dramatic differences among the phase-parameter sets at this energy with the possible exception of the  $\epsilon_1$  coupling parameter which is a factor of 2 lower in the Y-IV set than in the L and MS sets. The calculated curves at 330 MeV have the puzzling feature that the  $n$ -C curves show noticeable splitting among phase-parameter sets while the  $p$ -C curves do not. Even in these cases, however, the splitting due to various phase-parameter sets is considerably less than the splitting due to the different types of correlation function. This observation suggests that within the limitations of this approach,<sup>1,9</sup> calculations of this type might be useful in distinguishing among various types of nuclear correlation functions.

#### ACKNOWLEDGMENTS

We would like to acknowledge stimulating discussions with our colleague, Dr. Shi-Yu Wu. Thanks are also due to Robert Curry and David Senn of the University of Louisville Computer Center for assistance in converting the program for these calculations to the IBM 360/40 disk system, and to director Dr. John Sinai for making large amounts of computer time available to us.

<sup>1</sup>J. S. Chalmers and A. M. Saperstein, Phys. Rev. **168**, 1145 (1968).

<sup>2</sup>G. Breit, M. H. Hull, Jr., K. E. Lassila, K. D. Pyatt, Jr., and H. M. Ruppell, Phys. Rev. **128**, 826 (1962); M. H. Hull, Jr., K. E. Lassila, M. H. Ruppell, F. A. McDonald, and G. Breit, *ibid.*, **128**, 830 (1962).

<sup>3</sup>R. A. Arndt and M. A. MacGregor, Phys. Rev. **141**, 873 (1966).

<sup>4</sup>R. E. Seamon, K. A. Friedman, G. Breit, R. D. Haracz, J. M. Holt, and A. Prakash, Phys. Rev. **165**, 1579 (1968). Set Y-IV is used.

<sup>5</sup>M. H. MacGregor, R. A. Arndt, and R. M. Wright,

Phys. Rev. **173**, 1272 (1968). We use the single-energy sets with both singlet and triplet phases searched; referred to here as L-IX.

<sup>6</sup>M. H. MacGregor, R. A. Arndt, and R. M. Wright, Phys. Rev. **182**, 1714 (1969). The energy-independent phases are used and referred to as L-X.

<sup>7</sup>M. D. Miller, P. S. Signell, and N. R. Yoder, Phys. Rev. **176**, 1724 (1968). Set A is used and referred to as MS-A.

<sup>8</sup>K. M. Watson, Phys. Rev. **105**, 1388 (1957).

<sup>9</sup>J. S. Chalmers and A. M. Saperstein, Phys. Rev. **156**, 1099 (1967).

<sup>10</sup>R. R. Johnston and K. M. Watson, Nucl. Phys. **28**, 583 (1961).

<sup>11</sup>K. Brueckner and J. Gammel, Phys. Rev. **109**, 1023 (1958).

<sup>12</sup>D. Steinberg, J. N. Palmieri, and A. M. Cormack, Nucl. Phys. **56**, 46 (1964).

<sup>13</sup>C. P. Van Zyl, R. G. P. Voss, and R. Wilson, Phil. Mag. **1**, 1003 (1956).

<sup>14</sup>C. J. Batty, Nucl. Phys. **23**, 562 (1961).

<sup>15</sup>T. T. Thwaites, Ann. Phys. (N.Y.) **12**, 56 (1961).

<sup>16</sup>O. Chamberlain, E. Segre, R. D. Tripp, C. Wiegand, and T. Ypsilantis, Phys. Rev. **102**, 1659 (1956).

<sup>17</sup>A. Ashmore, D. S. Mather, and S. K. Sen, Proc. Phys. Soc. (London) **71**, 552 (1958).

<sup>18</sup>J. M. Dickson and D. C. Salter, Nuovo Cimento **6**, 235 (1957).

<sup>19</sup>B. H. Jarvis and B. Rose, Phys. Letters **15**, 271 (1965).

<sup>20</sup>E. M. Hafner, Phys. Rev. **111**, 297 (1958).

## Limiting Cross Sections for Fission Isomers with Nanosecond Lifetimes Produced in Heavy-Ion Reactions\*

Frank H. Ruddy, M. N. Nambodiri, and John M. Alexander

*Department of Chemistry, State University of New York at Stony Brook, Stony Brook, Long Island, New York 11790*

(Received 19 October 1970)

Targets of Pr, Ce, Nd, Ir, Au, and Pb have been bombarded with heavy ions in order to produce fission isomers with nanosecond lifetimes. In all cases, limits for detection were set which were much lower than the cross sections previously reported for these systems. It is concluded that fission isomerism was not observed in the previously reported experiments.

Recently it was reported<sup>1</sup> that fission with nanosecond lifetimes had been observed in a number of heavy-ion-induced reactions. The detection geometry had been designed to observe, in the same experiment, fission decay either from recoils in flight or from recoils collected on catchers a few cm from the target. The experiments that we now report were initiated as a study of the formerly reported fission isomers, but have led us instead to reexamine their existence.

The experimental arrangement is shown in Fig. 1. The heavy-ion beam of the Yale University heavy-ion linear accelerator was collimated to 4.8 mm before striking the target, which was placed in a 8.0-mm aperture. Track detectors of Lexan, mica, and Makrofol were placed on the target cover plate (1.6 mm thick). The Lexan and mica detectors were scanned for tracks with projected length  $>3.5 \mu$ . Therefore they were sensitive mainly to fission from recoils in flight that decayed at distances of between 5 and 20 mm downstream from the target.<sup>1</sup> The Makrofol detectors were scanned by a spark technique<sup>2</sup> that required incident angles of greater than  $\approx 45^\circ$  to the detector surface. Therefore, these detectors were sensitive both to fission decay from recoils in flight and also to decay from recoils collected on the catcher placed 15.9 cm downstream.

The Makrofol detectors of 5- $\mu$  thickness were etched for 6 h at 35°C in 6.2 N NaOH, and the microscopic holes, produced by fission fragments

impinging with angles greater than  $45^\circ$ , were developed to a diameter of  $\approx 50 \mu$  by spark scanning.<sup>2</sup> The resultant holes were observed with the aid of a microfilm reader-copier.

In the present series of experiments we have found disagreement with our previous results. When there were no catchers or baffles within about 5 cm of the target, we found upper limits for cross sections of delayed fission much lower than those previously reported.<sup>1</sup> A series of experiments ( $\text{Au}^{197} + 9\text{-MeV/amu B}^{11}$ ) were performed to determine the effect of the placement of catchers at varying distances from the target. As

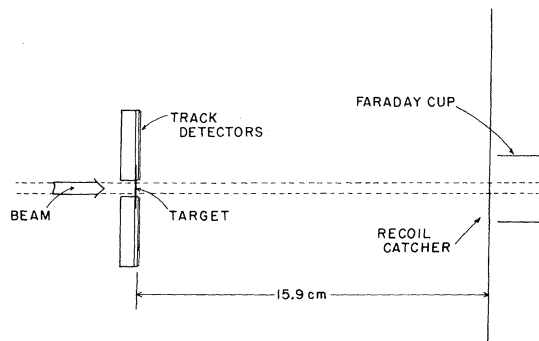


FIG. 1. Schematic diagram of the target and detector holder. Reaction products that recoil into the region in front of the target could undergo fission and yield tracks in the detectors placed in the position shown. The recoil catcher was Lexan foil of 0.08-mm thickness.